

A two-parameter mathematical model for immobilized enzymes and Homotopy analysis method

Rathinasamy Angel Joy¹, Athimoolam Meena², Shunmugham Loghambal², Lakshmanan Rajendran^{2*}

¹Department of Mathematics, Sri. G.V.G. Visalakshi College for women (Autonomous), Udumalpet, India;

²Department of Mathematics, The Madura College, Madurai, India; *Corresponding Author: raj_sms@rediffmail.com

Received 20 June, 2011; revised 4 July, 2011; accepted 10 July, 2011.

ABSTRACT

A two parameter mathematical model was developed to find the concentration for immobilized enzyme systems in porous spherical particles. This model contains a non-linear term related to reversible Michaelis-Menten kinetics. Analytical expression pertaining to the substrate concentration was reported for all possible values of Thiele module ϕ and α . In this work, we report the theoretically evaluated steady-state effectiveness factor for immobilized enzyme systems in porous spherical particles. These analytical results were found to be in good agreement with numerical results. Moreover, herein we employ new "Homotopy analysis method" (HAM) to solve non-linear reaction/diffusion equation.

Keywords: Mathematical Modeling; Michaelis-Menten Kinetics; Homotopy Analysis Method; Reaction/Diffusion Equation; Effectiveness factor

1. INTRODUCTION

The enzymes can be easily separated from the reaction bulk and reused by using immobilized enzymes on a porous support. Here the reaction occurs only inside the particle. Hence the external diffusion processes and diffusion within the particles affect the reaction rate. The internal diffusion effects can be quantitatively expressed by the effectiveness factor η (ratio of the average rate inside the particle to the rate in the absence of diffusional limitations). The mathematical models for estimating the effectiveness factor for heterogeneous enzymatic systems are developed on the basis of the following assumptions [1]. The catalytic particle is spherical and its radius is R , the enzyme is uniformly distributed throughout the whole catalytic particle, the enzyme reaction is mono substrate, the system is at steady-state and

is isothermal, the mass transfer resistance between solution and particle external surface is negligible, the substrate and product diffusion inside the catalytic particle can be modeled by the first Fick's law and the effective diffusivity does not change through out the particle.

In this assumption, a two-parameter model was proposed by Engasser and Horvath and this provides generalized plots of the effectiveness factor as a function of dimensionless modulus for the evaluation of simple Michaelis-Menten and product competitive inhibition kinetics. This model is used in the design of heterogeneous enzymatic reactors: fixed bed reactors [2] continuous tank reactors [3] and fluidized bed reactors [4]. The same model is used for the simulation of a packed bed immobilized enzyme reactor performing lactose hydrolysis.

Only numerical solutions were available for all the above said models since substrate concentration rate is a non-linear function of the substrate and product concentrations. More often finite differences [5] and orthogonal allocation [6] methods were used to solve the boundary value problem. Here as in enzymatic kinetics, the result is non linear equations system whenever the mass balance equations are non-linear. The solution may not be unique and can have convergence problem if finite differences were used [5]. The orthogonal allocation method is not reliable when high diffusional limitations occur because this method uses polynomial expressions to approach the concentration profiles [6]. To solve the boundary value problem Range Kutta method can also be used and here the initial substrate concentration is needed which is unknown. This can be calculated by successive calculations (shooting method) [7].

Analytical solutions have been obtained in the limiting cases of zero and first reaction order [8-10]. For the remaining, numerical calculus has been ordinarily used, being the different variables of the system expressed in dimensionless form [11-17]. The calculus complexity increases when the reaction mechanism is more complex [18,19] (Michaelis-Menten Kinetics). When reversible

or product competitive inhibition mechanisms have been considered, only external diffusional limitations [20] have been evaluated, otherwise unsatisfactory results were obtained [21-23].

Recently Gomez *et al.*, [1] presented the effectiveness factor of two-parameter model using Runge-Kutta method. However, to the best of author's knowledge, no general analytical results of substrate, product concentrations and effectiveness factor for immobilized enzyme on porous supports have been published. The purpose of this article is to derive steady state analytical expression of substrate, product concentration and the effectiveness factor using Homotopy analysis method (HAM).

2. FORMULATION OF THE BOUNDARY VALUE PROBLEM AND ANALYSIS

Figure 1 represents the schematic representation of the geometry adopted by spherical catalyst particle [1]. In general, it was assumed that in steady-state system the substrate and product diffusion inside the catalytic particle can be modeled by the first Fick's law and the effective diffusivity does not change through out the particle.

Under the above assumptions, the coupled differential equations for substrate and product in spherical co-ordinates are [1]:

$$\frac{D_s}{r^2} \frac{d}{dr} \left(r^2 \frac{dC_s}{dr} \right) = V_s \quad (1)$$

$$\frac{D_p}{r^2} \frac{d}{dr} \left(r^2 \frac{dC_p}{dr} \right) = -V_s \quad (2)$$

Now the boundary conditions are [1]

$$r = 0 \Rightarrow \frac{dC_s}{dr} = 0; \quad \frac{dC_p}{dr} = 0; \quad (3)$$

$$r = R \Rightarrow C_s = C_{SR}; C_p = C_{PR} \quad (4)$$

where reaction rate $V_s = \frac{V_m (C_s - (C_p/K_{eq}))}{K_m + C_s + (K_m/K_p)C_p}$.

Here C_s and C_p denote the dimensional substrate and product concentration, r is the radial co-ordinate, R denotes the radius of the particle, D_s and D_p are the diffusion-coefficients of the substrate and product respectively, C_{SR} and C_{PR} denote the local substrate and product concentration., K_{eq} is the reaction equilibrium constant, K_m is the Michaelies-Menten constant and V_m defines the maximum reaction rate. The form of V_s determines the mathematical method to solve the above equations and its complexity. Adding **Eqs.1** and **2** and using the boundary conditions given by **Eqs.3** and **4** the following relationship can be established:

$$C_p = C_{PR} + \frac{D_s}{D_p} (C_{SR} - C_s) \quad (5)$$

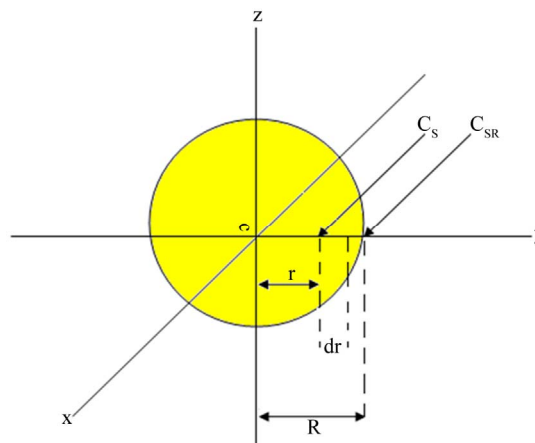


Figure 1. Schematic representation of the geometry adopted by spherical catalyst particle.

Substituting the value of C_p in V_s , we can obtain

$$V_s = \frac{V_m \left(1 + \frac{1}{K_{eq}} \frac{D_s}{D_p} \right) (C_s - C_{SE})}{K_M + \frac{K_M}{K_P} C_{PE} + C_{SE} + \left(1 - \frac{K_M}{K_P} \frac{D_s}{D_p} \right) (C_s - C_{SE})} \quad (6)$$

where $K_{eq} = \frac{C_{PE}}{C_{SE}}$,

$$C_{SE} = \frac{C_{PR} + (D_s/D_p)C_{PR}}{K_{eq} + (D_s/D_p)} \quad \text{and}$$

$$C_{PE} = K_{eq} C_{SE} = \frac{C_{PR} + (D_s/D_p)C_{PR}}{1 + (1/K_{eq})(D_s/D_p)}$$

We make the non-linear differential equations outlined in **Eqs.1** and **2** dimensionless by introducing the following dimensionless parameters:

$$U = \frac{C_s - C_{SE}}{C_{SR} - C_{SE}}, \quad \rho = \frac{r}{R},$$

$$\varphi = \frac{R^2 V_m}{(C_{SR} - C_{SE}) D_s} \left(1 + \frac{1}{K_{eq}} \frac{D_s}{D_p} \right) \left(1 - \frac{K_M}{K_P} \frac{D_s}{D_p} \right) \quad \text{and}$$

$$\alpha = \frac{K_M + \frac{K_M}{K_P} C_{PE} + C_{SE}}{(C_{SR} - C_{SE}) \left(1 - \frac{K_M}{K_P} \frac{D_s}{D_p} \right)} \quad (7)$$

where U represents the dimensionless substrate concentration, ρ denotes the dimensionless radius of the particle, φ and α denote the dimensionless modulus.

Now the **Eqs.1** and **2** reduces to the following dimensionless form [1] :

$$\frac{1}{\rho^2} \frac{d}{d\rho} \left(\rho^2 \frac{dU}{d\rho} \right) = \varphi \frac{U}{\alpha + U} \quad (8)$$

The boundary conditions are given by

$$\rho = 0; \frac{dU}{d\rho} = 0 \quad (9)$$

$$\rho = 1; U = 1 \quad (10)$$

The effectiveness factor is [1]

$$\eta = 3(\alpha + 1) \int_0^1 \frac{U}{U + \alpha} \rho^2 d\rho; \quad (11)$$

The set of expressions presented in **Eqs.9, 10** and **11** define the boundary value problem.

3. HOMOTOPY ANALYSIS METHOD

Liao [24] proposed a powerful analytical method for nonlinear problems, namely the Homotopy analysis method (see Appendix A). Different from all reported perturbation and non-perturbative techniques, the Homotopy analysis method [25-30] itself provides us with a convenient way to control and adjust the convergence region and rate of approximation series, when necessary. Briefly speaking, the Homotopy analysis method has the following advantages: It is valid even if a given nonlinear problem does not contain any small/large parameters at all; It can be employed to efficiently approximate a nonlinear problem by choosing different sets of base functions. In this paper we employ HAM to give approximate analytical solutions of coupled non-linear reaction/diffusion **Eq.9**. Using Homotopy analysis method (see Appendix -A) we can obtain the following new approximate substrate concentration by solving the **Eq.9**.

$$U(\rho) = 1 - \frac{h\varphi}{6\alpha} (\rho^2 - 1) + \frac{h\varphi}{6\alpha^2} \left[\frac{h\varphi}{20} \rho^4 - \left((1+h)\alpha + h + \frac{\varphi h}{6} \right) \rho^2 + \left((1+h)\alpha + h + \frac{7h\varphi}{60} \right) \right] \quad (12)$$

Using **Eq.12**, we can obtain the effectiveness factors

$$\eta(\alpha, \varphi) = \frac{(\alpha + 1)}{\varphi h A} \cdot \left[\varphi h A + 18\alpha^2 (A - \varphi h B) - 108\alpha^3 B (1 + \alpha) \right] \quad (13)$$

$$A = \sqrt{\varphi^2 h^2 + 6\varphi h \alpha (\alpha + 1)} \quad (14)$$

where
and $B = \operatorname{arctanh} \left(\frac{\varphi h}{A} \right)$

Eqs.12 and **13** represent the new approximate analytical expression of substrate and effectiveness factor for all values of parameters

4. LIMITING CASES

4.1. Case I: First Order Catalytic Kinetics

In this case $\alpha \gg U$. Now the above **Eq.9** reduces to

$$\frac{1}{\rho^2} \frac{d}{d\rho} \left(\rho^2 \frac{dU}{d\rho} \right) = \frac{\varphi}{\alpha} U \quad (15)$$

Using reduction of order method we can obtain the substrate concentration as

$$U(\rho) = \frac{\sinh \left(\sqrt{\frac{\varphi}{\alpha}} \rho \right)}{\rho \sinh \left(\sqrt{\frac{\varphi}{\alpha}} \right)} \quad (16)$$

The effectiveness factor is

$$\eta = \frac{3(\alpha + 1)}{\varphi} \left(\sqrt{\frac{\varphi}{\alpha}} \coth \left(\sqrt{\frac{\varphi}{\alpha}} \right) - 1 \right) \quad (17)$$

4.2. Case II: Zero Order Catalytic Kinetics

In this case $\alpha \ll U$. Now the **Eq.9** reduces to

$$\frac{1}{\rho^2} \frac{d}{d\rho} \left(\rho^2 \frac{dU}{d\rho} \right) = \varphi \quad (18)$$

Solving **Eq.18**, we can obtain the concentration of the substrate as follows:

$$U(\rho) = 1 + \frac{1}{6} \varphi (\rho^2 - 1) \quad (19)$$

The effectiveness factor is

$$\eta = \frac{(\alpha + 1)}{\varphi \sqrt{l}} \left[\varphi \sqrt{l} - 18\alpha \sqrt{l} \left(1 - l \operatorname{arctanh} \left(\varphi / \sqrt{l} \right) \right) - 108\alpha \operatorname{arctanh} \left(\varphi / \sqrt{l} \right) (1 + \alpha) \right] \quad (20)$$

where $l = \varphi^2 - 6\varphi(\alpha + 1)$.

5. RESULTS AND DISCUSSION

Eqs.12 and **13** represent the analytical solution of the concentration of substrate and effectiveness factor respectively. The Thiele modulus φ can be varied by

changing either the particle radius or the amount of concentration of substrate. This parameter describes the relative importance of diffusion and reaction in the particle radius. When ϕ is small, the kinetics are the dominant resistance; The overall uptake of substrate in the enzyme matrix is kinetically controlled. Under these conditions, the substrate concentration profile across the membrane is essentially uniform. In contrast, when the Thiele modulus ϕ is large, diffusion limitations are the principal determining factor.

5.1. Numerical Simulation

The HAM provides an analytical solution in terms of an infinite power series. However, there is a practical need to evaluate this solution and to obtain numerical values from the infinite power series. The consequent series truncation and the practical procedure conducted to accomplish this task, together transforms the otherwise analytical results into an exact solution, which is evaluated to a finite degree of accuracy. In order to investigate the accuracy of the HAM solution with a finite number of terms, the system of differential equation were solved. To show the efficiency of the present method for our problem in comparison with the numerical solution (SCILAB program) we report our results graphically. The SCILAB program is also given in Appendix (C).

5.2. Comparison of Analytical and Numerical Results

Figures 2(a)-(c) show the dimensionless steady-state substrate concentration for the different values of ϕ calculated using Eq.13. From these figures, we can see that the value of the concentration increases when Thiele modulus ϕ decreases. The concentration of substrate $U(\rho)$ increases slowly and rises abruptly when $\rho \geq 0.4$ and all values of ϕ . When $\phi < 1$ and $\alpha \leq 5$ the concentration of substrate $U(\rho) \approx 1$ (steady-state value). When ϕ is small, the overall uptake of substrate in the enzyme matrix is kinetically controlled and the substrate concentration profile across the membrane is identical.

Figure 3 represents the effectiveness factor η versus dimensionless Thiele modulus ϕ for different values of dimensionless module α . From this figure, it is inferred that, a constant value of dimensionless module α , the effectiveness factor decreases quite rapidly as dimensionless module ϕ increases, approaching zero at high values, which corresponds to internal diffusion controlled processes. Moreover, it is also well known that, a constant value of dimensionless module ϕ , the

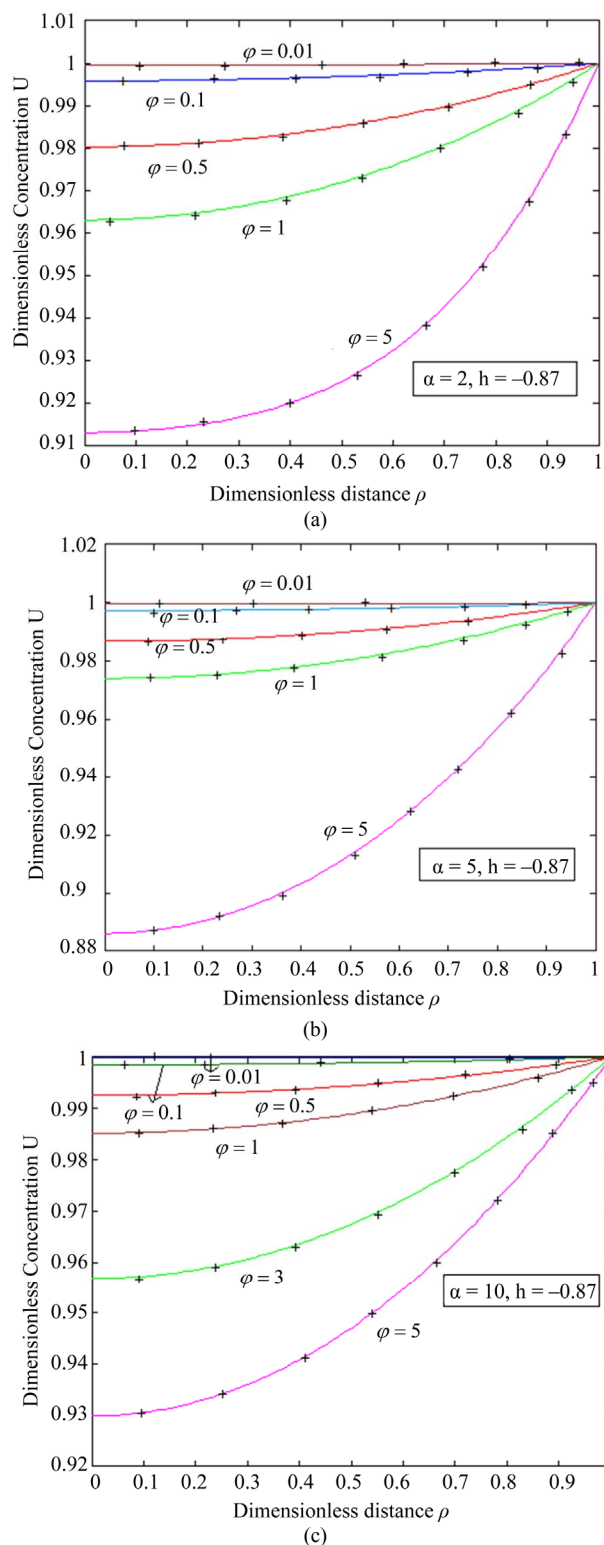


Figure 2. Comparison of normalized substrate concentration U versus normalized distance ρ for various values of Thiele modulus ϕ . (a) $\alpha = 2$ (b) $\alpha = 5$ (c) $\alpha = 10$. The curves are plotted using Eq. (13). (—) denotes the analytical results (+) denotes the numerical results. Here $h = -0.87$.

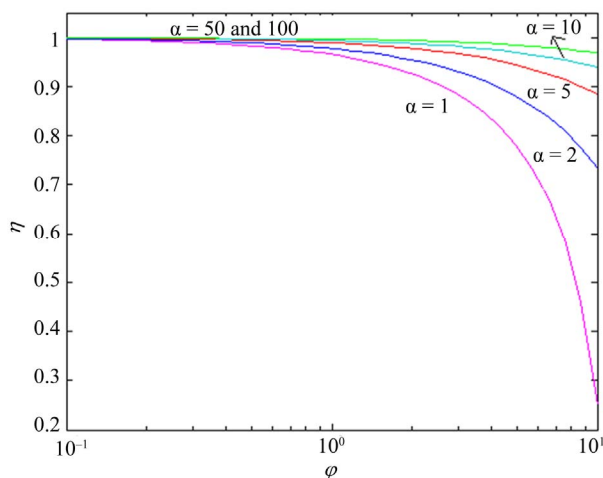


Figure 3. The normalized effectiveness factor η versus Thiele moduli ϕ for various values of parameter α . The curves are plotted using Eq.13. Here $h = -0.135$.

effectiveness factor increases with increasing values of α .

6. CONCLUSIONS

A non-linear time independent equation has been formulated and solved analytically using Homotopy analysis method. The primary result of this work is the first approximate calculations of substrate concentrations and effectiveness factor for non-linear Michaelis-Menten kinetic scheme. A simple closed form of analytical expressions of steady-state substrate and effectiveness factor are given. The analytical expressions for the substrate concentration profiles for all values of parameters α and ϕ are derived using Homotopy analysis method. This method is an extremely simple method and it is also a promising method to solve other non-linear equations. The extension of this procedure to other direct reaction of substrate at underlying microdisc electrode surface seems possible.

7. ACKNOWLEDGEMENTS

This work was supported by the Department of Science and Technology (DST) Government of India. The authors also thank Mr.M.S. Meenakshisundaram, Secretary, The Madura College Board, Principal and S.Thiagarajan Head of the Department of Mathematics, The Madura College, Madurai, India for their constant encouragement. It is our pleasure to thank the referees for their valuable comments.

REFERENCES

- [1] Gomez J.L., Bodalo A., Gomez E., Bastida J. and Maximo M.F. (2003) Two-parameter model for evaluating effectiveness factor for immobilized enzymes with reversible Michaelis-Menten kinetics. *Chemical Engineering Science*, **58**, 4287-4290.
- [2] Manjon A., Iborra J.L., Gomez J.L., Gomez E., Bastida J. and Bodalo A. (1987) Evaluation of the effectiveness factor along immobilized enzyme fixed-bed reactors: Design of a reactor with naringinase covalently immobilized into glycophasse-coated porous glass. *Biotechnology and Bioengineering*, **30**, 491-497. [doi:10.1002/bit.260300405](https://doi.org/10.1002/bit.260300405)
- [3] Bodalo S.A., Gomez C.J.L., Gomez E., Bastida R.J. and Martinez M. E. (1993) Transient stirred-tank reactors operating with immobilized enzyme systems: Analysis and simulation models and their experimental checking. *Biotechnology Progress*, **9**, 166-173. [doi:10.1021/bp00020a008](https://doi.org/10.1021/bp00020a008)
- [4] Bodalo A., Gomez J.L., Gomez E., Bastida J. and Maximo M.F. (1995) Fluidized bed reactors operating with immobilized enzyme systems: Design model and its experimental verification. *Enzyme and Microbial Technology*, **17**, 915-922. [doi:10.1016/0141-0229\(94\)00125-B](https://doi.org/10.1016/0141-0229(94)00125-B)
- [5] Carnahan B., Luther H.A. and Wilkes J.O. (1969) Applied numerical methods, Wiley, New York.
- [6] Villadsen J., Michelsen M.L. (1978) Solution of differential equation models by polynomial approximation. New York: Prentice-Hall, Englewood Cliffs.
- [7] Lee J. and Kim D.H. (2005) An improved shooting method for computation of effectiveness factors in porous catalysts. *Chemical Engineering Science*, **60**, 5569-5573. [doi:10.1016/j.ces.2005.05.027](https://doi.org/10.1016/j.ces.2005.05.027)
- [8] Lyons M.E.G., Greer J.C., Fitzgerald C.A., Bannon T. and Bartlett P.N. (1996) Reaction/Diffusion with Michaelis-Menten kinetics in electroactive polymer films Part 1. The steady-state amperometric response. *Analyst*, **12**, 1715.
- [9] Lyons M.E.G., Bannon T., Hinds G. and Rebouillat S. (1998) Reaction/Diffusion with Michaelis-Menten kinetics in electroactive polymer films Part 1. The transient amperometric response. *Analyst*, **123**, 1947. [doi:10.1039/a803274b](https://doi.org/10.1039/a803274b)
- [10] Lyons M.E.G., Murphy J., Bannon T. and Rebouillat S. (1999) Reaction, diffusion and migration in conducting polymer electrodes: Analysis of the steady-state amperometric response. *Journal of Solid State Electrochemistry*, **3**, 154-162. [doi:10.1007/s100080050142](https://doi.org/10.1007/s100080050142)
- [11] Moo-Young M. and Kobayashi T. (1972) Effectiveness factors for immobilized enzyme reactions. *Canadian Journal of Chemical Engineering*, **50**, 162-167. [doi:10.1002/cjce.5450500204](https://doi.org/10.1002/cjce.5450500204)
- [12] Kobayashi T. and Laidler K. J. (1973) Effectiveness factor calculations for immobilized enzyme catalysts. *Biochimica et Biophysica Acta*, **1**, 302-311.
- [13] Engasser J.M. and Horvath J.C. (1973) Metabolism: interplay of membrane transport and consecutive enzymic reaction. *Journal of Theoretical Biology*, **42**, 137-155. [doi:10.1016/0022-5193\(73\)90153-7](https://doi.org/10.1016/0022-5193(73)90153-7)
- [14] Marsh D.R., Lee Y.Y. and Tsao G.T. (1973) Immobilized glucoamylase on porous glass. *Biotechnology and Bioengineering*, **15**, 483-492. [doi:10.1002/bit.260150305](https://doi.org/10.1002/bit.260150305)
- [15] Hamilton B.K., Cardner C.R. and Colton C.K. (1974) Effect of diffusional limitations on lineweaver-burk plots for immobilized enzymes. *AIChE Journal*, **20**, 503-510.

- [doi:10.1002/aic.690200310](https://doi.org/10.1002/aic.690200310)
- [16] Rovito B.J. and Kittrell J.R. (1973) Film and pore diffusion studies with immobilized glucose Oxidase. *Biotechnology and Bioengineering*, **15**, 143-161. [doi:10.1002/bit.260150111](https://doi.org/10.1002/bit.260150111)
- [17] Engasser J.M. (1978) The experimental results accorded quantitatively with the theory of diffusion limitation. *Biochimica et Biophysica Acta*, **526**, 301-310.
- [18] Aydogan O., Bayraktar E. and Mehmetoglu U. (2011) Determination of effective diffusion coefficient of acetophenone in carrageenan and asymmetric bioreduction in packed bed reactor. *Journal of Molecular Catalysis B: Enzymatic*, **72**, 46-52. [doi:10.1016/j.molcatb.2011.04.023](https://doi.org/10.1016/j.molcatb.2011.04.023)
- [19] Puida M., Malinauskas A., Ivanauskas F. (2011) Modeling of electrocatalysis at conducting polymer modified electrodes: Nonlinear current-concentration profiles. *Journal of Mathematical chemistry*, **49**, 1151-1162. [doi:10.1007/s10910-011-9802-y](https://doi.org/10.1007/s10910-011-9802-y)
- [20] Marc A. and Engasser J.M. (1982) Influence of substrate and product diffusion on the heterogeneous kinetics of enzymic reversible reactions. *Journal of Theoretical Biology*, **94**, 179-189. [doi:10.1016/0022-5193\(82\)90339-3](https://doi.org/10.1016/0022-5193(82)90339-3)
- [21] Goldman R., Keden O., Silman I.H., Caplan S.R. and Katchalski E. (1968) Papain-collodion membranes. I. Preparation and properties. *Biochemistry*, **7**, 486-500. [doi:10.1021/bi00842a002](https://doi.org/10.1021/bi00842a002)
- [22] Engasser J.M. and Horvath C. (1974) Inhibition of bound enzymes. II. characterization of product inhibition and accumulation. *Biochemistry*, **133**, 849-3854.
- [23] Ramachandran P.A. (1975) Solution of immobilized enzyme problems by collocation methods. *Biotechnology and Bioengineering*, **17**, 211-226. [doi:10.1002/bit.260170207](https://doi.org/10.1002/bit.260170207)
- [24] Liao S.J. (1992) The proposed homotopy analysis technique for the solution of nonlinear problems, Ph. D. Thesis, Shanghai Jiao Tong University, Shanghai.
- [25] Awawdeh F., Jaradat H.M. and Alsayyed O. (2009) Solving System of DAEs by Homotopy Analysis. *Chaos Solitons and Fractals*, **42**, 1422-1427. [doi:10.1016/j.chaos.2009.03.057](https://doi.org/10.1016/j.chaos.2009.03.057)
- [26] Jafari H., Chun C., Seifi S. and Saeidy M., (2009) Analytical solution for nonlinear Gas Dynamic equation by Homotopy Analysis Method. *Applied Mathematics*, **4**, 149-154.
- [27] Sohoul A.R., Famouri M., Kimiaefar A. and Domairry G., (2010) Application of homotopy analysis method for natural convection of Darcian fluid about a vertical full cone embedded in porous media prescribed surface heat flux. *Communications in Nonlinear Science and Numerical Simulation*, **15**, 1691-1699. [doi:10.1016/j.cnsns.2009.07.015](https://doi.org/10.1016/j.cnsns.2009.07.015)
- [28] Domairry G. and Fazeli M. (2009) Homotopy analysis method to determine the fin efficiency of convective straight fins with temperature-dependent thermal conductivity. *Communications in Nonlinear Science and Numerical Simulation*, **14**, 489-499. [doi:10.1016/j.cnsns.2007.09.007](https://doi.org/10.1016/j.cnsns.2007.09.007)
- [29] Liao S.J. (2004) On the homotopy analysis method for nonlinear problems. *Applied Mathematics and Computation*, **147**, 499-513. [doi:10.1016/S0096-3003\(02\)00790-7](https://doi.org/10.1016/S0096-3003(02)00790-7)
- [30] Domairry G. and Baramia H. (2008) An Approximation of the Analytic Solution of Some Nonlinear Heat Transfer Equations: A Survey by using Homotopy Analysis Method. *Advanced studies in Theoretical Physics*, **2**, 507-518.
- [31] Liao S.J. (2003) Beyond Perturbation: Introduction to the Homotopy analysis method. Chapman and Hall, CRC Press, Boca Raton. [doi:10.1201/9780203491164](https://doi.org/10.1201/9780203491164)

APPENDIX A

Basic Idea of Liao’s [31] Homotopy Analysis method

Consider the following differential **Eq.31**:

$$N[u(t)] = 0 \tag{A1}$$

where, N is a nonlinear operator, t denotes an independent variable, $u(t)$ is an unknown function. For simplicity, we ignore all boundary or initial conditions, which can be treated in the similar way. By means of generalizing the conventional homotopy method, Liao constructed the so-called zero-order deformation equation as:

$$(1-p)L[\varphi(t;p) - u_0(t)] = pH H(t) N[\varphi(t;p)] \tag{A2}$$

where $p \in [0,1]$ is the embedding parameter, $h \neq 0$ is a nonzero auxiliary parameter, $H(t) \neq 0$ is an auxiliary function, L is an auxiliary linear operator, $u_0(t)$ is an initial guess of $u(t)$ and $\varphi(t;p)$ is an unknown function. It is important, that one has great freedom to choose auxiliary unknowns in HAM. Obviously, when $p = 0$ and $p = 1$, it holds:

$$\varphi(t;0) = u_0(t) \text{ and } \varphi(t;1) = u(t) \tag{A3}$$

respectively. Thus, as p increases from 0 to 1, the solution $\varphi(t;p)$ varies from the initial guess $u_0(t)$ to the solution $u(t)$. Expanding $\varphi(t;p)$ in Taylor series with respect to p , we have:

$$\varphi(t;p) = u_0(t) + \sum_{m=1}^{+\infty} u_m(t) p^m \tag{A4}$$

where

$$u_m(t) = \frac{1}{m!} \left. \frac{\partial^m \varphi(t;p)}{\partial p^m} \right|_{p=0} \tag{A5}$$

If the auxiliary linear operator, the initial guess, the auxiliary parameter h , and the auxiliary function are so properly chosen, the series **Eq.A4** converges at $p = 1$ then we have:

$$u(t) = u_0(t) + \sum_{m=1}^{+\infty} u_m(t). \tag{A6}$$

Define the vector

$$\mathbf{u}_n = \{u_0, u_1, \dots, u_n\} \tag{A7}$$

Differentiating **Eq.A2** for m times with respect to the embedding parameter p , and then setting $p = 0$ and finally dividing them by $m!$, we will have the so-called m^{th} -order deformation equation as:

$$L[u_m - \chi_m u_{m-1}] = hH(t) \mathfrak{R}_m(\mathbf{u}_{m-1}) \tag{A8}$$

where

$$\mathfrak{R}_m(\mathbf{u}_{m-1}) = \frac{1}{(m-1)!} \left. \frac{\partial^{m-1} N[\varphi(t;p)]}{\partial p^{m-1}} \right|_{p=0} \tag{A9}$$

and

$$\chi_m = \begin{cases} 0, & m \leq 1, \\ 1, & m > 1. \end{cases} \tag{A10}$$

Applying L^{-1} on both side of **Eq.A8**, we get

$$u_m(t) = \chi_m u_{m-1}(t) + hL^{-1}[H(t) \mathfrak{R}_m(\mathbf{u}_{m-1})] \tag{A11}$$

In this way, it is easy to obtain u_m for $m \geq 1$, at M^{th} order, we have

$$u(t) = \sum_{m=0}^M u_m(t) \tag{A12}$$

when $M \rightarrow +\infty$, we get an accurate approximation of the original **Eq.A1**. For the convergence of the above method we refer the reader to Liao [31]. If **Eq.A1** admits unique solution, then this method will produce the unique solution. If **Eq.A1** does not possess unique solution, the HAM will give a solution among many other (possible) solutions.

APPENDIX B

$$\frac{1}{\rho^2} \frac{d}{d\rho} \left(\rho^2 \frac{dU}{d\rho} \right) = \varphi \frac{U}{\alpha + U} \tag{B1}$$

Now the boundary conditions become

$$\rho = 0, \frac{dU}{d\rho} = 0 \tag{B2}$$

$$\rho = 1, U = 1 \tag{B3}$$

In order to solve **Eq.B1** by means of the HAM, we first construct the Zeroth-order deformation equation by taking $H(t) = 1$,

$$\begin{aligned} (1-p) \left(\alpha \frac{d^2 \delta}{d\rho^2} + \frac{2\alpha}{\rho} \frac{d\delta}{d\rho} \right) &= \\ = pH \left((\alpha + \delta) \left(\frac{d^2 \delta}{d\rho^2} + \frac{2}{\rho} \frac{d\delta}{d\rho} \right) - \varphi \delta \right) \end{aligned} \tag{B4}$$

subject to the boundary conditions

$$\delta'(0;p) = 0,$$

$$\delta(1;p) = 1 \tag{B5}$$

where $p \in [0,1]$ is an embedding parameter and $h \neq 0$ is the so-called convergence control parameter. When $p = 0$

$$\frac{d^2 \delta(\rho;0)}{d\rho^2} + \frac{2}{\rho} \frac{d\delta(\rho;0)}{d\rho} = 0 \tag{B6}$$

From **Eq.B6** we get

$$\delta_0 = 1 \quad (\text{B7})$$

When $p = 1$ the **Eq.B4** is equivalent to **Eq.B1**, thus it holds

$$\delta(\rho; 1) = U(\rho) \quad (\text{B8})$$

Expanding $\delta(\rho; p)$ in Taylor series with respect to the embedding parameter p , we have,

$$\delta(\rho; p) = U_0(\rho) + \sum_{m=1}^{+\infty} U_m(\rho) p^m \quad (\text{B9})$$

where

$$U_0(\rho) = \delta(\rho; 0) \quad (\text{B10})$$

and $U_m(\rho)$ ($m = 1, 2, \dots$) will be determined later. Note that the above series contains the convergence control parameter h . Assuming that h is chosen so properly that the above series is convergent at $p = 1$. We have the solution series as

$$U(\rho) = U_0(\rho) + \sum_{m=1}^{+\infty} U_m(\rho) \quad (\text{B11})$$

where

$$U_m(t) = \frac{1}{m!} \left. \frac{\partial^m U(\rho; p)}{\partial p^m} \right|_{p=0} \quad (\text{B12})$$

substituting **Eq.B9** into the zeroth-order deformation **Eqs.B4** and **B5** and equating the co-efficient of the like powers of p we have,

$$p^1 : \alpha \left(\frac{d^2 \delta_1}{d\rho^2} + \frac{2}{\rho} \frac{d\delta_1}{d\rho} \right) - [\alpha(1+h) + \delta_0 h] \quad (\text{B13})$$

$$\left(\frac{d^2 \delta_0}{d\rho^2} + \frac{2}{\rho} \frac{d\delta_0}{d\rho} \right) + h\phi\delta_0 = 0$$

$$p^2 : \alpha \left(\frac{d^2 \delta_2}{d\rho^2} + \frac{2}{\rho} \frac{d\delta_2}{d\rho} \right) - [\alpha(1+h) + \delta_0 h] \quad (\text{B14})$$

$$\left(\frac{d^2 \delta_1}{d\rho^2} + \frac{2}{\rho} \frac{d\delta_1}{d\rho} \right) - h\delta_1 \left(\frac{d^2 \delta_0}{d\rho^2} + \frac{2}{\rho} \frac{d\delta_0}{d\rho} \right) + h\phi\delta_1 = 0$$

and so on. From **Eqs.B13** and **B14** we get

$$\delta_1 = -\frac{h\phi}{6\alpha} (\rho^2 - 1) \quad (\text{B15})$$

$$\delta_2 = \frac{h\phi}{6\alpha^2} \left[\frac{h\phi}{20} \rho^4 - \left(\alpha(1+h) + h + \frac{\phi h}{6} \right) \rho^2 + \left(\alpha(1+h) + h + \frac{7\phi h}{60} \right) \right] \quad (\text{B16})$$

Adding **Eqs.B7**, **B15** and **B16** we get **Eq.13** in the text.

APPENDIX C

Determining the Region of h for Validity

The analytical solution should converge. It should be noted that the auxiliary parameter h controls the convergence and accuracy of the solution series. The analytical solution represented by **Eq.13** contains the auxiliary parameter h , which gives the convergence region and rate of approximation for the homotopy analysis method. In order to define region such that the solution series is independent of h , a multiple of h -curves are plotted. The region where the distribution of U and U' versus h is a horizontal line is known as the convergence region for the corresponding function. The common region among the $U(\rho)$ and its derivatives are known as the overall convergence region. To study the influence of h on the convergence of solution, the h -curves of $U(0.5)$ and $U'(0.5)$ are plotted in **Figures 4(a)** and **(b)** respectively, for $\phi = 5$ and $\alpha = 10$. These figures clearly indicate that the valid region of h is about $-1 < h < -0.8$. Similarly we can find the value of the convergence control parameter h for different values of constant parameters.

APPENDIX D

function pdex1

$m = 2;$

$x = \text{linspace}(0,1);$

$t = \text{linspace}(0,100);$

$\text{sol} = \text{pdepe}(m, @pdex1pde, @pdex1ic, @pdex1bc, x, t);$

% Extract the first solution component as u.

$u = \text{sol}(:, :, 1);$

% A surface plot is often a good way to study a solution.

$\text{surf}(x, t, u)$

$\text{title}(\text{Numerical solution computed with 20 mesh points.})$

$x \text{ label}(\text{Distance } x')$

$y \text{ label}(\text{Time } t')$

% A solution profile can also be illuminating.

figure

$\text{plot}(x, u(\text{end}, :))$

$\text{title}(\text{'Solution at } t = 2')$

$x \text{ label}(\text{Distance } x')$

$y \text{ label}(u(x, 2)')$

% -----

function [c,f,s] = pdex1pde(x,t,u,DuDx)

$c = 1;$

$f = \text{DuDx};$

$k = 0.01;$

$\text{alpha} = 0.5;$

$s = -k * u / (\text{alpha} + u);$

% -----

function u0 = pdex1ic(x)

$u0 = 1;$

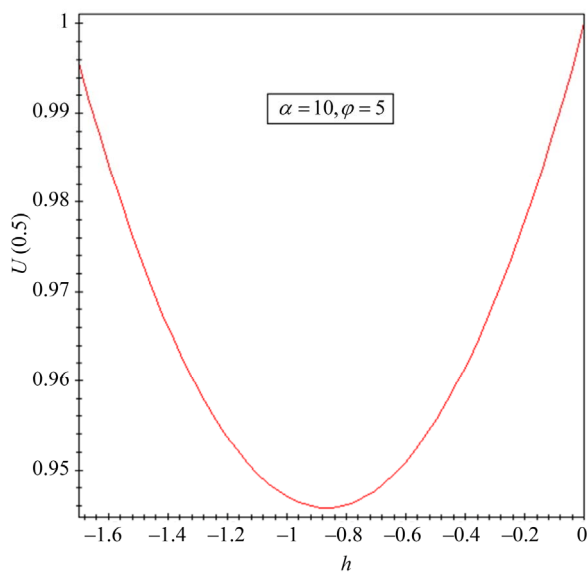
% -----

function [pl,ql,pr,qr] = pdex1bc(xl,ul,xr,ur,t)
 pl = 0;
 ql = 1;
 pr = ur-1;
 qr = 0;

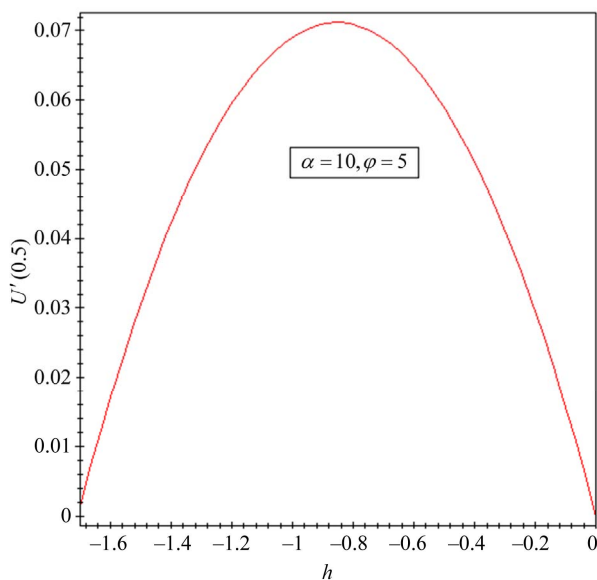
APPENDIX E

Consider

$$\frac{1}{\rho^2} \frac{d}{d\rho} \left(\rho^2 \frac{dU}{d\rho} \right) = \frac{\varphi}{\alpha} U \tag{E1}$$



(a)



(b)

Figure 4. The *h* curves to indicate the convergence region, for $\varphi = 5$ and $\alpha = 10$.

Boundary conditions are:

$$\begin{aligned} \rho = 1; \quad U = 1, \\ \rho = 0; \quad \frac{dU}{d\rho} = 0. \end{aligned} \tag{E2}$$

Using reduction of order, we have

$$P = \frac{2}{\rho}; \quad Q = \frac{\varphi}{\alpha}; \quad R = 0. \tag{E3}$$

Let

$$U = uv \tag{E4}$$

Substitute **Eq.E4** in **Eq.E1** and choose *u* such that

$$2 \frac{du}{d\rho} + Pu = 0$$

Substituting the value of *P*, we obtain

$$u = \frac{1}{\rho} \tag{E5}$$

Now the **Eq.E1** reduces to

$$v'' + Q_1 v = R_1 \tag{E6}$$

$$Q_1 = Q - \frac{1}{2} \frac{dP}{d\rho} - \frac{\rho^2}{4} = \frac{\varphi}{\alpha}, \quad R_1 = \frac{R}{u} = 0 \tag{E7}$$

Substituting **Eq.E7** in **Eq.E6** we obtain

$$v'' - \frac{\varphi}{\alpha} v = 0. \tag{E8}$$

Solving we obtain

$$v = Ae^{\sqrt{\frac{\varphi}{\alpha}}\rho} + Be^{-\sqrt{\frac{\varphi}{\alpha}}\rho}. \tag{E9}$$

Substituting **Eq.E5** and **Eq.E9** in **Eq.E4** we have

$$U = \frac{1}{\rho} \left(Ae^{\sqrt{\frac{\varphi}{\alpha}}\rho} + Be^{-\sqrt{\frac{\varphi}{\alpha}}\rho} \right) \tag{E10}$$

Using the boundary conditions we obtain the value of the constants as

$$A = \frac{1}{2 \sinh\left(\sqrt{\frac{\varphi}{\alpha}}\right)}; \quad B = -\frac{1}{2 \sinh\left(\sqrt{\frac{\varphi}{\alpha}}\right)} \tag{E11}$$

Substituting in **Eq.E10** we obtain the solution as

$$U = \frac{\sinh\left(\sqrt{\frac{\varphi}{\alpha}}\rho\right)}{\rho \sinh\left(\sqrt{\frac{\varphi}{\alpha}}\right)} \tag{E12}$$

Appendix F

Nomenclature and Units	
Symbols	
C_S	Concentration of the substrate ($\text{mol}\cdot\text{cm}^{-3}$)
C_P	Concentration of the product ($\text{mol}\cdot\text{cm}^{-3}$)
r	Radial co-ordinate (cm)
C_{SR}	Local substrate concentration ($\text{mol}\cdot\text{cm}^{-3}$)
C_{PR}	Local product concentration ($\text{mol}\cdot\text{cm}^{-3}$)
K_{eq}	Reaction equilibrium constant (none)
K_m	Michaelis-Menten constant ($\text{mol}\cdot\text{cm}^{-3}$)
D_S	Diffusion coefficient of the substrate ($\text{cm}^2\cdot\text{sec}^{-1}$)
D_P	Diffusion coefficient of the product ($\text{cm}^2\cdot\text{sec}^{-1}$)
R	Radius of the particle (cm)
V_S	Local reaction rate per unit of catalytic particle volume ($\text{mol}\cdot\text{cm}^{-3}\cdot\text{s}^{-1}$)
V_m	Maximum reaction rate per unit of catalytic particle volume ($\text{mol}\cdot\text{cm}^{-3}\cdot\text{s}^{-1}$)
U	Normalized substrate concentration (none)
φ, α	Normalized Thiele modulus (none)
η	Effectiveness factor (none)